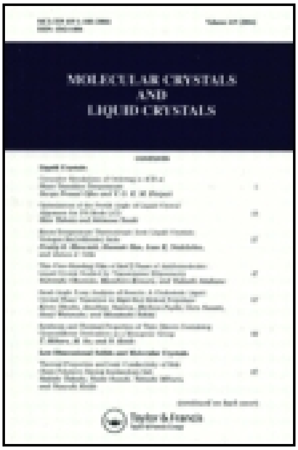

Molecular Crystals and Liquid Crystals Science and Technology. Section A. Molecular Crystals and Liquid Crystals

Angle-Resolved, Resonance-and Inverse-Photoemission Studies of Transition Metal Intercalated TiS^2

Shigemasa Suga [a]

[a] Graduate School of Engineering Science, Osaka University, Toyonaka, Osaka, 560-8531, Japan

Version of record first published: 27 Oct 2006

To cite this article: Shigemasa Suga (2000): Angle-Resolved, Resonance-and Inverse-Photoemission Studies of Transition Metal Intercalated TiS^2 , Molecular Crystals and Liquid Crystals Science and Technology. Section A. Molecular Crystals and Liquid Crystals, 341:2, 9-14

To link to this article: http://dx.doi.org/10.1080/10587250008026109

Mol. Cryst. and Liq. Cryst., 2000, Vol. 341, pp. 9-14
Reprints available directly from the publisher
Photocopying permitted by license only

Published by license under the
Gordon and Breach Science Publishers imprint.
Printed in Malaysia

Angle-Resolved, Resonance- and Inverse-Photoemission Studies of Transition Metal Intercalated TiS_2

SHIGEMASA SUGA

Graduate School of Engineering Science, Osaka University, Toyonaka, Osaka 560–8531, Japan

Electronic structures of transition metal intercalated 1T-TiS_2, M_xTiS_2, are studied by means of angle resolved photoemission, Ti 2p photoabsorption, 2p XPS, 2p resonance valence photoemission and ultraviolet inverse photoemission spectroscopy. Dispersions of the valence bands are noticeably modified from the host 1T-TiS_2. Several new features are interpreted and importance of the electron correlation and hybridization effects is confirmed.

Keywords: M_xTiS_2; XPS; core resonance; angle-resolved photoemission; band structures

INTRODUCTION

3d transition metal(M) intercalated 1T-TiS_2, M_xTiS_2(M=Mn, Fe, Co and Ni), show various unusual properties, depending on the guest atom species and its concentration[1]. In $M_{1/3}TiS_2$, the intercalant M atoms occupy the nearly octahedral interstitial sites in the van der Waals gap between the neighboring sulfur layers and a $\sqrt{3}a \times \sqrt{3}a$ triangular-super lattice is formed. On the other hand, $M_{1/4}TiS_2$ has a 2x2 super lattice. Band structures of $M_{1/3}TiS_2$ were calculated by the augmented-plane-wave(APW) method[2]. Gross valence band features were discussed from the 3p→3d resonance photoemission[3]. XPS of core-levels and valence bands were also performed[4]. Although the band density of states (DOS) was already studied for $M_{1/3}TiS_2$ by UPS and XPS, details of the band dispersions and symmetries of electronic states are not yet fully clarified. We report on angle-resolved ultraviolet-photoemission(ARUPS), 2p core absorption(XAS), 2p→3d resonance photoemission(RPES) and vacuum ultraviolet inverse photoemission(IPES) on M_xTiS_2 in comparison with 1T-TiS_2.

EXPERIMENTAL

Samples were cleaved in an ultra-high vacuum chamber. The crystal orientation was determined either by LEED or by RHEED. ARUPS was performed with using synchrotron radiation at BL-18A of the Photon Factory (PF) with the angular resolution of ±1°and energy resolution of 300 meV. The analyzer was rotated in the horizontal plane for the polar angle (θ) scanning while $h\nu$ was fixed at 28eV. The normal photoemission spectra ($\theta = 0°$) were measured with changing $h\nu$. The 2p XAS and 2p→3d RPES were performed at BL-2B of PF. IPES was performed at 9.4 eV. All measurements were performed at room temperature. The Fermi energy E_F was calibrated..

RESULTS AND DISCUSSION

Angle Resolved Photoemission, Inverse Photoemission and Band Dispersions

ARUPS spectra and dispersions of occupied bands were already reported for 1T-TiS_2(hereafter abbreviated as TiS_2) by several authors.[5] Typical ARUPS spectra are shown for $Co_{1/3}TiS_2$ in Fig.1 for (a)Γ(A)-M(L) and (b) Γ(A)-K(H) axes. Dispersions are shown in Fig.2(b) in comparison with TiS_2 in Fig.2(a).

A strong band is observed just below E_F in $Co_{1/3}TiS_2$ in Fig.1(a) in the θ range of 20-40° near the M(L) point. This structure K is observed in a wide wave vector region(the symbol A is used to emphasize the strong region in Fig.2(b)). The band K is observed for all M_xTiS_2, whereas its intensity is weaker for x=1/4 than for x=1/3. Its origin is clarified later from Ti 2p RPES. Only in Ni_xTiS_2, the intensity of the band K is also noticeably enhanced near the Γ point on the Γ(A)-M(L) as well as Γ(A)-K(H) axes. This behavior may be related to the hole like conductivity in $Ni_{1/3}TiS_2$.

Another feature in $Co_{1/3}TiS_2$ is an appearance of a new band L near E_B=0.5 eV. Although any corresponding feature is absent in $Mn_{1/4}TiS_2$ and $Fe_{1/3}TiS_2$, a similar structure is observed near E_B=1 eV in $Ni_{1/3}TiS_2$ and $Ni_{1/4}TiS_2$. It is clear that structure L is related to the M 3d state. The dispersion of this structure L is very weak along the Γ(A)-M(L), Γ(A)-K(H) as well as Γ-A axes, clarifying rather localized character. M 3d states are split into the "t_{2g}" and "e_g" states. The "t_{2g}" states consist of three base functions. Although they hardly make bonding states with the S atoms, the d_{z2} state(here z refers to the crystallographic axis perpendicular to the TiS_2 layer) faces toward the upper and the lower Ti atoms making the bonding and antibonding states. These states are not band states but have a localized character, because the distance between the equivalent bonding states along the z axis is very large. Thus L is interpreted as the M $3d_{z2}$-Ti$3d_{z2}$ bonding state.

In regard to most other bands in M_xTiS_2, one recognizes counterparts in TiS_2. Inhomogenious energy shifts and splittings of various bands clarify the

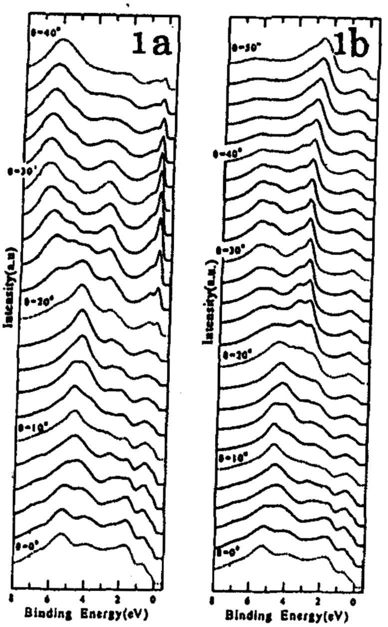

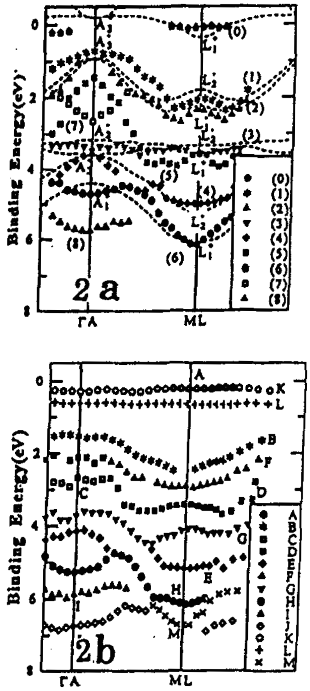

FIGURE 1 ARUPS of $Co_{1/3}TiS_2$ along (a)Γ(A)-M(L) and (b) Γ(A)-K(H) at hν=28 eV.

FIGURE 2 Band dispersions in (a)1T-TiS_2 and (b)$Co_{1/3}TiS_2$ along the Γ(A)-M(L) axis. The dashed curves in (a) is the result of band calculation for the A-L axis.[6]

breakdown of the rigid-band shift model. Although the bands D and H are thought to correspond to the bands 5 and 6 in TiS_2, which have the S 3pπ character and remarkable dispersion for $k_{//}$ and $k_{\perp}$, the effect of intercalation is noticeable and suggests appreciable hybridization with the M 3d "e_g" states. The broader peak width may be also resulting from the hybridization effect. The bands B and E are thought to correspond to the bands 2(or 1) and 4 in TiS_2. Broadening of these bands is not much different from TiS_2, suggesting that the hybridization effect with the M 3d states is weak. Meanwhile, the bands G and F are thought to correspond to the bands 3 and 1(or 2). They are strongly modified by the intercalation. The broadening of them is more than that of the bands 3 and 1(or 2), being subjected to the strong hybridization. Thus half of the S 3pσ bands (B and E) is hardly influenced by the intercalation, whereas the other half(G and F) is thought to be well hybridized with the M 3d "e_g" states. The increase of the whole valence band width is very clear in M_xTiS_2 in consistence with the result of band calculation.[2]

Normal incidence(θ=0°) IPES spectra are then measured to probe the unoccupied states as summarized in Fig.3. Two groups of structures are observed in 0-2 and 2-4 eV above E_F corresponding to the t_{2g} and e_g related bands. Since the Ti 3d states are almost empty in contrast to the more than half occupation of the M 3d states and the concentration of M is rather low, the IPES spectral shape mostly reflects the Ti 3d empty states and is not sensitive to the M 3d states. As for the Ti "e_g" band in M_xTiS_2, the center of gravity is found to be slightly in the lower energy region than TiS_2. The "t_{2g}" spectra have shown a low energy component in $Mn_{1/4}TiS_2$ and $Fe_{1/3}TiS_2$, which may suggest the Ti d_{z2}-M d_{z2} bonding state. The anti-bonding Ti d_{z2}-M d_{z2} state in $Co_{1/3}TiS_2$ and $Ni_{1/3}TiS_2$ may be overlapping with the main "t_{2g}" band and is not discriminated.

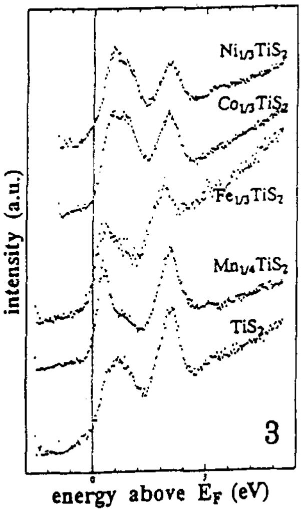

FIGURE 3 Vacuum ultraviolet inverse photoemission specra.

Ti 2p XPS, 2p Core Absorption and 2p Resonance Photoemission

XPS spectra were measured for Ti 2p core level. Satellite structures are observed at ~10 eV larger E_B. Defining the charge transfer(CT) energy Δ as $E(d^2L)-E(d^1)$, where L denotes a ligand hole, the energy splitting of the 2p core photoemission final states is represented as $[(\Delta-U_{dd}-U_{dc})^2+4V_{eff}^2]^{1/2}$ according to a simple configuration interaction analysis assuming the d^0 and d^1L final states. Here U_{dd} is the correlation energy, U_{dc} is the Coulomb attraction energy and V_{eff} is the hybridization energy. By assuming Δ=4.5~5 eV, U_{dd}=4 eV, U_{dc}=6 eV, V_{eff} is estimated to be ~4.5 eV. It is found that the main peak is much broadened in M_xTiS_2 compared with TiS_2, because it is composed of both "well screened" and "poorly screened" components.

Ti 2p XAS were measured by means of the total photoelectron yield as shown in Fig.4. Clear four peak structure is observed for TiS_2, where the spin-orbit splitting corresponds to the energy separation between 1and 3(or 2 and 4) components. The crystal field splitting of the 3d state roughly corresponds to the splitting between the components 1 and 2(or 3 and 4). In higher hv region is observed a weak satellite S. The spectrum in TiS_2 resembles those in nominally tetravalent(d^0) TiO_2 and $SrTiO_3$. In the simple configuration interaction analysis, the splitting between the main peak and the CT satellite is estimated as $[(\Delta-U_{dc})^2+4V_{eff}'^2]^{1/2}$ for the $\underline{2p}3d^1$ and $\underline{2p}3d^2\underline{L}$ configurations. From the observed splitting of 8.5 eV, V_{eff}' is estimated as ~4.2 eV. The lowest energy peak is predicted to be a single line by full-multiplet CT(charge transfer) theory.

The spectra of M_xTiS_2 are very similar among different M but remarkably different from that of TiS_2. The structures 1 and 3 become rather inconspicuous. The spectra resemble that of VO_2 with d^1 nominal configuration. The spectra are considered to be mainly resulting from the strong hybridization between the $\underline{2p}3d^2$ and $\underline{2p}3d^3\underline{L}$ configurations. Still the charge transfer satellite is observed.

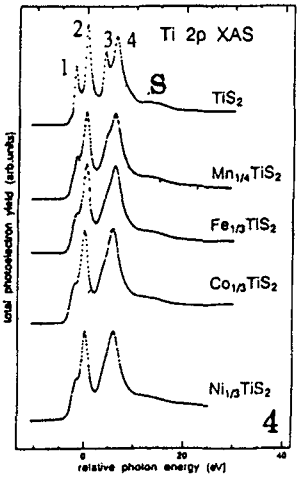

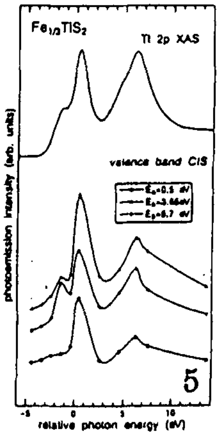

FIGURE 4 Ti 2p core absorption(XAS) spectra.

FIGURE 5 Constant initial state spectra of $Fe_{1/3}TiS_2$. The behavior of K is represented for E_B=0.5 eV considering the resolution.

Valence band spectra for 2p resonance excitation were measured in the form of the constant initial state spectra(CIS). A typical result of $Fe_{1/3}TiS_2$ for Ti 2p core excitation is shown in Fig.5. The structure K is strongly enhanced for the excitation to the "e_g" state. Enhancement for the "t_{2g}" excitation is much weaker. Similar behavior is observed for all M_xTiS_2 and suggests Ti "e_g" like character of K rather than the "t_{2g}" like character in contrast to our supposition. This discrepancy can be solved by considering a system with Ti $3d^1$ ground state, which is made by the charge transfer from M to Ti atom in M_xTiS_2. The real ground state can be represented by a linear combination of the $d^1(t_{2g})$ and $d^2(t_{2g},e_g)L$ states. The photoemission final state is given by a linear combination of d^0, $d^1(t_{2g})L$ and $d^1(e_g)L$ states. The observed resonance for the Ti 2p→e_g excitation is attributed to the $d^1(t_{2g})L$ final state realized after emitting the e_g electron in the direct recombination process. As for the structure L in $Ni_{1/3}TiS_2$ with weak dispersion, no resonance enhancement is observed for e_g excitation. Such a behavior is consistent with its interpretation as the Ti $t_{2g}d_{z^2}$-Ni $t_{2g}d_{z^2}$ hybridized state. A prominent L_3VV Auger feature is observed in the valence band region of M_xTiS_2 in contrast to TiS_2, suggesting the d^1 character in the ground state. In all M_xTiS_2, a satellite enhancement is also recognized near E_B=8.5 eV. This is ascribed to the charge transfer satellite resulting from the d^0 and d^1L final states resulting from the d^1 and d^2L initial states.

In conclusion, the electronic states of M_xTiS_2 were studied in comparison with 1T-TiS_2 by means of various photon and electron spectroscopy. Both band structures and correlated electron states are clarified. New features observed in various spectra are interpreted and hybridization effects between M 3d, Ti 3d and S 3p states are confirmed

Acknowledgments

The author acknowledges Dr.T.Matsushita, Prof.A.Kimura, Mr.T.Terauchi, Prof. H.Negishi and Prof.M.Inoue for fruitful collaborations. This work was supported by a Grant-in-Aid for COE research(Grant No.10CE 2004) of the Ministry of Education, Science, Sports and Culture, Japan.

References

[1] M. Inoue, Y. Muneta, H. Negishi and M. Sasaki, J. Low Temp. Phys., **63**, 235 (1986) and references therein.
[2] N. Suzuki, T. Yamazaki and K. Mochizuki, J. Phys. Soc. Jpn **58**, 3280 (1989) and references therein.
[3] Y. Ueda, K. Fukushima, H. Negishi, M. Inoue, M. Taniguchi and S. Suga, J. Phys. Soc. Jpn., **56**, 2471 (1987).
[4] A. Fujimori, S. Suga, H.Negishi and M. Inoue, Phys. Rev. B **38**, 3676 (1988).
[5] J. J. Barry, H. P. Hughes, P. C. Klipstein and R. H. Friend, J. Phys. C **16**, 393 (1983).
[6] A. Zunger and A. J. Freeman, Phys. Rev. B**16**, 906 (1977).